# Physics of Near-Source Strong Ground Motions

*Kazuki Koketsu[1]

1. Earthquake Research Institute, University of Tokyo

Several theories have been proposed for the cause of near-source strong ground motion. Among them, the rupture directivity effect is one that has been long studied and widely accepted. Its physics is clear and the mechanism described in this theory is that seismic ground motions radiated from subfaults along the progress of fault rupture yield a strong ground motion in the direction of rupture propagation due to constructive interference. Meanwhile, the fling step effect has also been proposed, but its physics is unclear. It is written that “The other (cause) is due to the movement of the ground associated with the permanent offset of the ground” in Bolt and Abrahamson (2003). However, since both the permanent offset and strong ground motion are results of earthquake faulting, one of them cannot be a cause of the other. Also, as Hisada (2003) showed without intention, they are naturally contained in seismic ground motions calculated from earthquake faulting. If we dare to distinguish it as a special one, it can be related to the near-field term of seismic ground motion that contributes greatly near the source region. Nevertheless, it is necessary to present a reason if the near-field term becomes strong ground motion. In addition, it has been explained that the earthquake faulting motion itself appears in seismic ground motion. There is no objection on this explanation, but this can apply to all kinds of seismic ground motion, because all of them are the results of earthquake faulting. Therefore, this cannot explain why strong ground motion occurs, like the fling step effect.

It has been thought that rupture directivity occurs if a strike-slip or dip-slip rupture propagates to a site in the along-strike or updip direction, respectively. Its effects appear in the fault-normal component of seismic ground motion. However, though the 2015 Gorkha earthquake was a dip-slip event, the along-strike rupture propagation generated large ground motion pulses. For the 2016 Kumamoto earthquake, large ground motion pulses were found in the fault-parallel component. Accordingly, the fling step effect and faulting motion theory have been advocated, but our studies showed the rupture directivity effect to be a main cause of the large pulses. The first key point is that a ‘large’ ground motion pulse has to occur for the identification of rupture directivity. Although constructive interference can occur in any rupture direction, a large ground motion pulse is not generated if subfaults along the direction radiate only small ground motions or their focal mechanisms vary largely. For a typical dip slip of 45 degree, large ground motions are not generated along the strike direction because of a nodal plane in the S-wave radiation pattern, and therefore, the rupture directivity is not visible during the along-strike rupture propagation of a typical dip-slip earthquake. Since the Gorkha earthquake is a low-angle dip-slip event of 10 degree, the strike direction got away from the nodal plane and into a zone of large ground motion in the radiation pattern, causing the rupture directivity effect. The second key point is that an overall rupture direction is not always similar to the rupture direction around a zone of large slip. The Kumamoto earthquake is this case so that the upward rupture propagation around its large-slip zone generated directivity pulses in the fault-parallel component.

To compare the rupture directivity and fling step contributions to ground motions in the near field of the Gorkha earthquake, we calculated ground motions using the far- and intermediate-field terms, or only the near-field term of the analytical solution in an infinite medium. The results of this calculation in the figure show that, even in the near field, the rupture directivity effect is mostly larger than the fling step effect. It is noted the most that the shape of a fling step pulse is mainly controlled by constructive interference like

©2017. Japan Geoscience Union. All Right Reserved. 

a rupture directivity pulse.

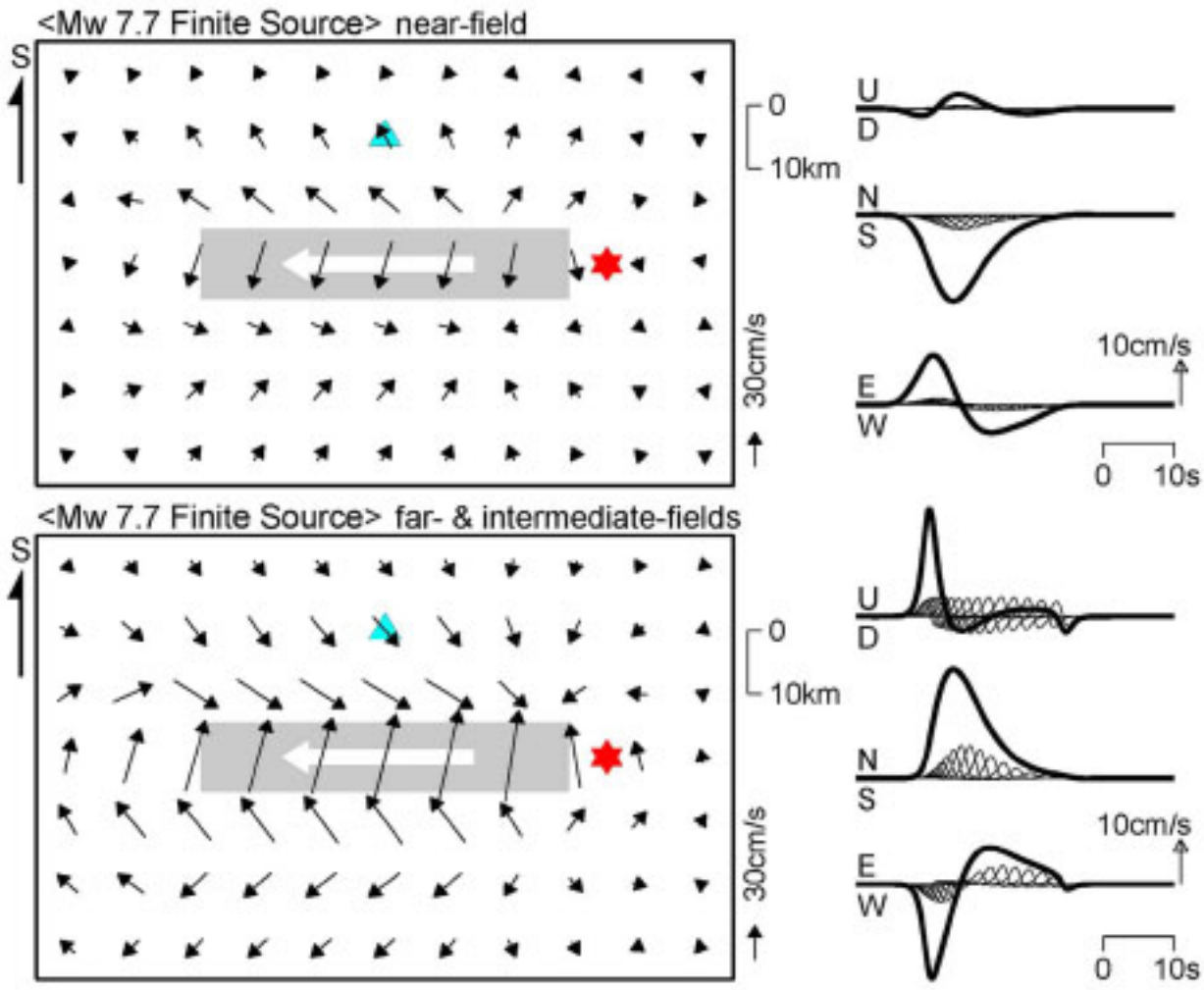


©2017. Japan Geoscience Union. All Right Reserved. 

# Characteristics of strong ground motion generation areas inferred from fully dynamic multicycle earthquake simulations

Percy Galvez[1], Paul Somerville[1], *Anatoly Petukhin[2], Ken Miyakoshi[2], Jean-Paul Ampuero[3], Yingdi Luo[3]

1. AECOM, United States, 2. Geo-Research Institute, Japan, 3. California Institute of Technology, United States

There is vast evidence that the fault regions that generate short-period and long-period wave radiation during a given earthquake can be spatially distinct. The most direct observations of this phenomenon have been obtained for large subduction earthquakes (e.g. 2011 Mw 9.0 Tohoku) for which the high frequency ground motion radiation has been detected in deep regions of seismogenic zones, while long-period ground motion are in shallow regions. In contrast, for moderate-size crustal events (Mw6-7) kinematic finite source models reveal that regions of large final slip (long-period generation areas) and regions of large peak slip velocity (short-period generation areas) spatially coincide. The phenomenon does not appear to be systematic for large Mw8 earthquakes. This feature has important implications on procedures adopted for the prediction of strong ground motion and need detailed study.

One plausible explanation for the discrepancy between short-period and long-period generation areas is based on the spatial heterogeneity of stress and strength (frictional parameters) along the fault. In fundamental models of earthquake dynamics, high-frequency radiation is generated by abrupt changes of rupture speed. High frequency radiation is also enhanced by short rise time which can be controlled by heterogeneous frictional velocity-weakening.

One fundamental goal of dynamic source modelling has been to design a class of spatial distributions of friction parameters that can be tuned to reproduce the statistical features of past earthquakes. An inherent difficulty in this effort was that stress and strength heterogeneities cannot be prescribed arbitrarily as was done in earlier work. Their inter-dependence must be consistent with a mechanical model of deformation and stress evolution over the longer time scale of the earthquake cycle. Failure to account for such mechanical correlations leaves the modeling framework so unconstrained that virtually any outcome is possible with sufficient tuning. For this reason we have developed the software infrastructure to simulate multiple earthquake cycles with rate-and-state friction, in which we solve consistently for long and short time scales of the earthquake cycle, combining periods of quasi-static and fully dynamic deformation.

With the benefit of the optimized software framework, we run simulations of a M8 vertical strike-slip fault. We associated the slip weakening Dc distribution with different degrees of fault maturity. Large variations of Dc represent immature faults and lower variations of Dc represent mature faults. We impose a lognormal distribution of Dc that correlates in space and defined two fault cases where fault case 1 has lower Dc variability (sigma = 0.25, mature fault) whereas fault case 2 has larger Dc variability (sigma = 1.0, immature fault). We examine the distinct locations of areas of large slip and large slip velocity. The analysis of the discrepancy of short-period and long-period generation areas has been supported by analysis of other dynamic quantities, including rupture speed, rise time and general attributes of band-passed filtered slip velocity time histories. With simulation results at hand (for peak slip and peak slip rate distributions slip see example below) we conclude that asperity area and high slip velocity area tend to be similar for Case 1 (mature faults), but occur in different places for Case 2 (immature faults). We found that high slip rate areas correspond to short rise time and high rupture velocity areas.

©2017. Japan Geoscience Union. All Right Reserved. 

Acknowledgement. This study was based on the 2016 research project 'Improvement for uncertainty of strong ground motion prediction' by the Nuclear Regulation Authority (NRA), Japan.

Keywords: strong ground motion, multicycle earthquake rupture modelling, fully dynamic simulation

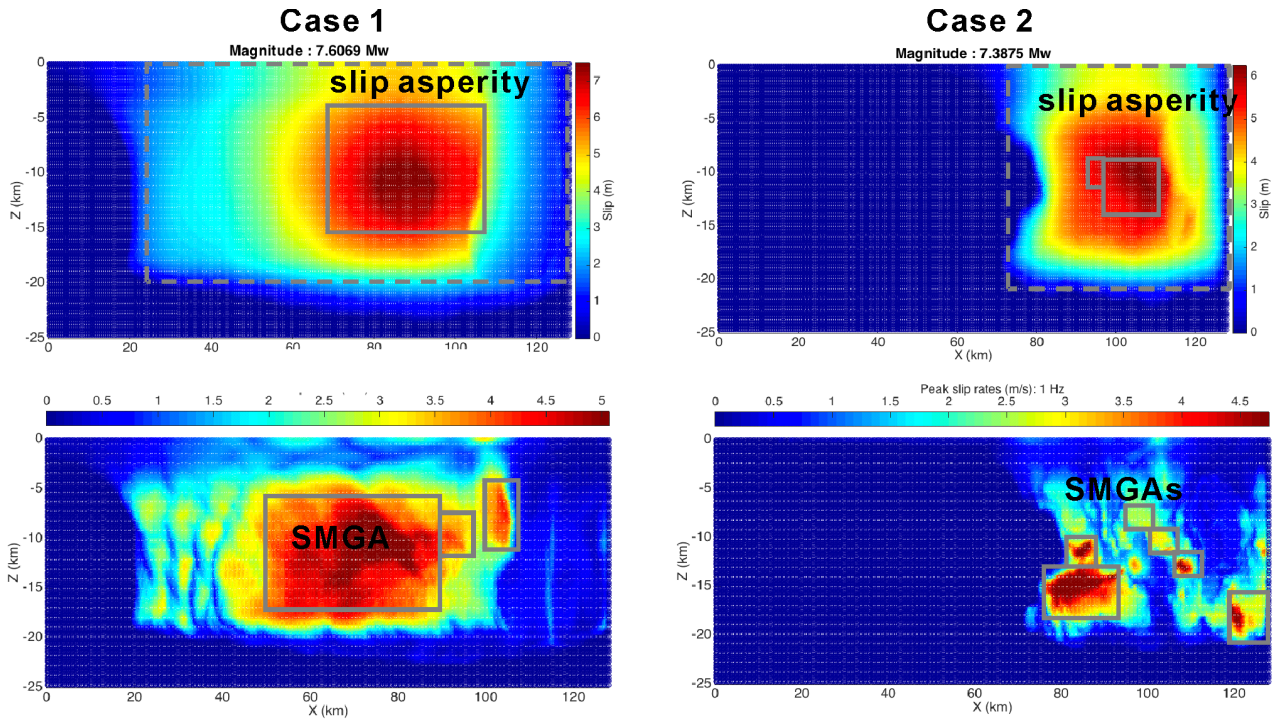


©2017. Japan Geoscience Union. All Right Reserved. 

# Analyzing Strong Motion Generation Area of the $M_{JMA}$ 6.5 Earthquake Occurring Offshore the Kii Peninsula on April 1, 2016

*Kimiyuki Asano[1]

1. Disaster Prevention Research Institute, Kyoto University

An $M_{JMA}$ 6.5 earthquake occurring along the Nankai trough is thought to be a thrust-event on the plate boundary between the Eurasian and Philippines Sea plates, where future mega-thrust earthquake is expected (e.g., Wallace *et al.*, 2016). Since this type of earthquake with moderate-to-large size is very rare in this region in the last half century, it is a good opportunity to investigate the source characteristics relating to strong motion generation of subduction-zone plate-boundary earthquakes in the Nankai area, southwest Japan.
We collected from near-source strong motion data recorded by accelerometers at cabled sea-floor stations of Dense Oceanfloor Network system for Earthquake and Tsunamis (DONET1) jointly operated by NIED and JAMSTEC. We also collected records from Long Term Borehole Monitoring System (LTBMS) installed within accretionary prism underling the Kumano sedimentary basin at a depth of 904 m below the see floor at site C0002, which is operated by JAMSTEC. In addition to offshore stations, we collected strong motion data from velocity-type strong motion sensors (VSE-355G3) recorded at onshore broadband stations in the Kii peninsula belonging to the F-net of NIED and those recorded at a station in Shionomisaki installed by DPRI, Kyoto University.
Beside the $M_{JMA}$ 6.5 mainshock, there are several M3 class aftershocks on the day of the mainshock. Firstly, we analyzed source spectral ratio between the mainshock and an EGF event to obtain the corner frequencies and the source scaling parameters for both events. We referred to the relocated catalog by Wallace *et al.* (2016) for the hypocenters of the mainshock and aftershocks. Then, we estimated the source parameters of strong motion generation area (SMGA) of this event based on broadband strong motion modeling by the empirical Green’s function method (Irikura, 1986; Miyake *et al.*, 2003) using both offshore and onshore strong motion stations. We will compare the source characteristics of this event with those from subduction-zone plate-boundary earthquakes in northeast Japan to discuss the regional difference in source characteristics in terms of strong motion generation from plate-boundary earthquakes.
Acknowledgements: We used strong motion data from Dense Oceanfloor Network system for Earthquake and Tsunamis (DONET) jointly operated by NIED and JAMSTEC, Long Term Borehole Monitoring System (LTBMS) of JAMSTEC, F-net broadband seismograph network of NIED, and DPRI, Kyoto University.

Keywords: strong motion generation area, plate-boundary earthquake, Nankai trough

©2017. Japan Geoscience Union. All Right Reserved. 

# UCSB Method for Broadband Ground Motion Prediction from Heterogeneous Earthquake Ruptures

*Ralph J Archuleta[1], Jorge Crempien[2,1]

1. University of California Santa Barbara, 2. Pontificia Universidad Católica de Chile

The UCSB method simulates earthquakes as heterogeneous kinematic ruptures to produce synthetic broadband ground motions (0-25Hz) for 5 **M** 8. A Kostrov-like slip-rate function is specified at a dense number of points on a finite fault. Each slip-rate function is specified by the total slip, time to reach the maximum slip-rate (peak-time), the total time of slipping (rise-time), and a rupture time, i.e., the time when the point first begins to slip. The rupture time is related to the local rupture velocity. The slip, peak time, rise time and rupture time are all characterized by their own marginal distribution (one-point statistic), and each parameter is correlated with the other. The heterogeneity of the slip distribution on the fault is determined by filtering white noise with a Von Karman wavenumber power spectrum. The Von Karman spectrum is determined from a correlation length and a spectral decay parameter for length scales shorter than the correlation length. The other kinematic parameters are also heterogeneous with different decay parameters--each functionally related to the decay of the slip. With a fault area and seismic moment (magnitude) the only remaining free parameter is average stress drop. The code will iterate on the kinematic parameters until the moment-rate spectrum of the simulated earthquake is similar to a Brune spectrum, with a low frequency level corresponding to the seismic moment and the corner frequency corresponding to the average stress drop.

We separate wave propagation at 1.0 Hz into low- and high-frequency components. The low-frequency ground motion is propagated using either a 1D or 3D velocity structure. The high-frequency Green's functions are computed for a layer over halfspace. The high-frequency amplitude is modified using the quarter-wavelength method using the detailed 1D velocity model of the velocity structure. The resulting high-frequency Green´s functions are then convolved with scattering functions, which are consistent with observed regional coda waves. We then merge the low- and high-frequency ground motion by stitching them in the wavelet domain. It is important to note that in the UCSB method, both the high- and low-frequency ground motion comes from a single source description even if the wave propagation is different.

We have successfully validated our method against well-recorded data produced by earthquakes in different tectonic regions such as California, eastern United States, and Japan. The validation metrics are bias between observed and synthetic acceleration response spectrum and direct comparison with ground motion prediction equations.

Keywords: Ground Motion, Earthquake, Heterogeneous Rupture

©2017. Japan Geoscience Union. All Right Reserved. 

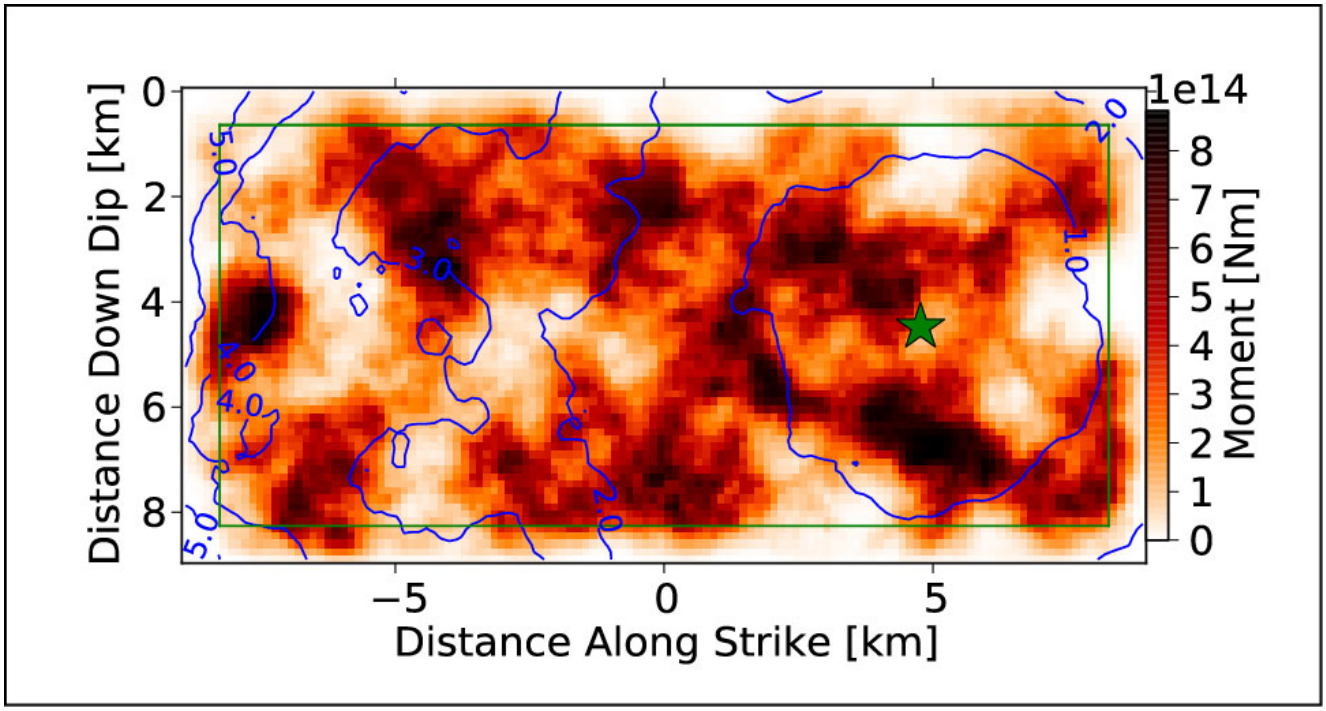


©2017. Japan Geoscience Union. All Right Reserved. 

# Characteristics of Near Fault Strong Ground Motion in the Kathmandu Valley during the 2015 Gorkha Nepal earthquake

*Nobuo TAKAI[1], Michiko Shigefuji[2], Subeg Bijukchhen[1], Masayoshi Ichiyanagi[1], Tsutomu Sasatani[1]

1. Hokkaido University, 2. Kyushu University

On 25 April 2015, a large Mw 7.8 earthquake occurred along the Main Himalayan Thrust fault in central Nepal. The epicenter was near the Gorkha region, 80 km north-west of the Kathmandu Valley, and the rupture propagated eastward from the epicentral region passing through the Kathmandu Valley. We have installed a strong motion array observation (four sites; one rock site and three sedimentary sites) in the Valley, on 20 September 2011, to understand the site effects of the Valley. We discuss the characteristics of near fault strong ground motion in the Kathmandu Valley during the 2015 Gorkha earthquake based on the strong motion records captured by this array.

The horizontal velocities waveforms on sedimentary sites are strongly affected by site amplification due to soft soil deposit and valley response (Takai et al. 2016; Galetzka et al. 2015). The velocity waveforms for the N207E (fault normal direction) and UD components observed at the rock site KTP show the distinguishing velocity pulse ground motions. They show a single-sided velocity pulse with a width of about 6 s, while the N117E (fault parallel direction) component show a double-sided pulse with a period of about 10 s. This N117E pulse is considered to be effect of along-strike directivity (Mavroeidis and Papageorgiou 2003), and the pulse shape was explained by the joint inversion result for rupture process (Kobayashi et al. 2016). The ground velocities at KKN4 obtained from the high-rate (5 Hz sampling) GPS record (Galetzka et al. 2015) have the similar waveforms as observed at KTP, while the amplitudes of the KKN4 velocity pulses are about 1.4 times larger than those of the KTP velocity pulses; KKN4 is a rock site located northwest of the Kathmandu Valley.

The Kathmandu Valley is located at a very close distance (~10 km) to the rupture area and the estimated large slip areas exist near the Valley. Furthermore, the displacement waveforms derived from the velocity pulses for the N207E and UD components at KTP show a monotonic step. These facts demonstrate the observed velocity pulses are effect of a permanent tectonic offset (Mavroeidis and Papageorgiou 2003). If the records are affected by the permanent tectonic offset, the velocity waveforms are similar to the slip-rate functions (Hisada and Bielak 2003). Galetzka et al. (2015) estimated the regularized Yoffe slip-rate time function from the vertical velocity waveform at KKN4 by forward modeling. They also showed that the estimated slip-rate time function well explained the vertical velocity waveforms at two stations in the Kathmandu Valley. We confirmed that the estimated slip-rate time function well explained the vertical velocity waveforms at our four stations. It is interesting to extract the slip-rate time function from the observed records without waveform modeling. We made a trial of extraction of the slip-rate time function based on the low-pass filtered acceleration waveform for vertical component at KTP; the cut-off frequency of the filter is 0.3Hz. The velocity and displacement waveforms obtained by single and double time-integration of the low-pass filtered accelerations show the velocity pulse and the monotonic step, respectively. We also confirmed the Fourier spectral shape at the low-frequency range (0.02-0.3Hz) of our low-pass filtered acceleration waveform is similar to that of the differentiated Yoffe slip-rate time function estimated by Galetzka et al. (2015).

Kamai et al. (2014) developed an empirical parametric model for the fling-step components based on an extensive set of finite-fault simulations. We compare the width of the velocity pulse (about 6 s) observed at KTP with their regression model of the period of the fling-step pulse for the reverse fault. The width of velocity pulse at KTP, is nearly the same as the median value of the regression model by Kamai et al.

©2017. Japan Geoscience Union. All Right Reserved. 

(2014). This means that the Gorkha earthquake with Mw 7.8 is normal one with respect to the fling-step motion.

Keywords: Fling-Step, permanent tectonic offset, Site Amplification

©2017. Japan Geoscience Union. All Right Reserved. 

# Long-period strong ground motions near the source fault of the 2016 Kumamoto earthquake

*Kojiro Irikura[1], Susumu Kurahashi[1]

1. Aichi Institute of Technology

## Introduction

The 2016 Kumamoto earthquake with Mw 7.0 occurred at 01:25JST on April 16, 2016 along the Futagawa fault zone and the northern part of the Hinagu fault zone. Surface breaks caused by the mainshock were found associated with Futagawa-Hinagu fault system by field surveys. Near-field strong ground motions with high accuracy during the 2016 Mw 7.0 Kumamoto earthquake were recorded by the NIED strong motion network (K-NET and KiK-net) and the JMA and local-government seismic-intensity network. In particular, two stations at Mashiki Town-Hall (MTH) and Nishihara Village-Hall (NVH) were located within 2 km of the surface traces along the Futagawa fault zone. The ground motions of the 2016 Kumamoto earthquake were well simulated using a characterized source model consisting of strong motion generation areas (SMGAs) based on the empirical Green's function (EGF) method except the very-near-field ground motions at MTH and NVH. We attempt to simulate the very-near-field ground motions with fling steps taking long-period generation areas (LMGAs) above the SMGAs into account.

## SMGA model for simulating strong ground motions of the 2016 Kumamoto earthquake

Many studies of slip distributions obtained from the waveform inversion of the strong-motion data for this event have so far been published (e.g., Asano and Iwata 2016; Kubo et al. 2016; Yoshida et al. 2016). The rupture area and asperity area were determined based on the slip distributions obtained from the waveform inversions of the strong motion observations. Irikura et al. (2017) found that the relationship between the rupture area and the seismic moment for this event follows the second-stage scaling relation within one standard deviation developed by Irikura and Miyake (2001). Characterized source models with the SMGAs are estimated, based on the slip distribution models of Yoshida et al. (2016) and Kubo et al. (2016). There are found two best-fit source models, both of which show a good agreement between synthetic and observed motions (Irikura et al., 2017). One is Model A with three SMGAs from Yoshida et al. (2016) and the other is Model B with a single SMGA from Kubo et al. (2016). The SMGA of Model B is located around a center of the three SMGAs of Model A. The combined area of three SMGAs of Model A is nearly equal to the area of the single SMGA of Model B. The ratio of the SMGA area to the total rupture area is 0.22–0.24. Then, the stress parameter of each SMGA is about 14 MPa.

## Long-period ground motions at very-near surface-fault stations

The ground motions at MTH and NVH show clearly the fling steps as shown in near-field ground motions during the 1992 Landers earthquake (Hisada and Bielak, 2003). The fling effects are dominant in the slip direction only in the vicinity of the surface fault and are negligible for buried faults, because the near-field terms of the Green's functions attenuates rapidly with distance from the fault, r, as the order of $(1/r^2)$. Therefore, the effects might have a strong influence on the ground motions at MTH and NVH, whereas less on those at KMMH16 and KMM006. We estimate the ground motions at MTH and NVH putting a long-period motion generation area (LMGA) between surface fault and the top of the seismogenic zone above the SMGA. We assume a long-period (about 3 s) modified-ramp-functions as slip velocity time functions on the LMGA, because the slip velocity time functions from the inversion results are expressed to be a bell shape near the surface fault, while they are Kostrov-type on deeper SMGAs, as shown in Kubo et al. (2016). The location of the LMGA is put near large slip from the inversion results. The area of the LMGA and the peak velocity of the slip velocity time function were determined through comparison between the synthetic and observed long-period motions. The synthetic ground motions as a sum of

©2017. Japan Geoscience Union. All Right Reserved. 

ground motions from the SMGA and those from the LMGA agree well with the observed motions with fling steps.

Keywords: 2016 Kumamoto earthquake, strong ground motion, near-field ground motions, lomg-period strong ground motions, fling steps

©2017. Japan Geoscience Union. All Right Reserved. 

# Ground Motion Simulation for Finite Faults using the Ambient Seismic Field

*Hiroe Miyake[1], Loic Viens[2], Marine A Denolle[2]

1. The University of Tokyo, 2. Department of Earth and Planetary Sciences, Harvard University

After the 2011 Tohoku earthquake, the Japanese government re-evaluated the source regions of potential megathrust earthquakes, leading to new seismic and tsunami hazards that need to be assessed. The long-period ground motions, which may affect tall-buildings and critical structures, need to be carefully simulated. Deterministic numerical simulation of long-period ground motions are currently widely applied for both crustal and subduction earthquakes. However, the period-range is limited between 1 to 20 s and 2 to 20 s for crustal and subduction earthquakes, respectively, due to the accuracy of the velocity structure models. As an alternative approach, ground motion simulation using the ambient seismic field (i.e., seismic interferometry) has been proposed.

Finite fault application is necessary for ground motion simulations of large magnitude earthquakes. Denolle et al. (2014) demonstrated the finite fault application of the ambient seismic field by simulating the ground motions of earthquake scenarios along the San Andreas fault. Simulated ground motions tend to over predict the ground motion obtained with physics-based simulations, indicating a possibility of large ground motion variations. Viens et al. (2016) showed a good agreement between observed and simulated ground motions for the 2008 Iwate-Miyagi earthquake. Surprisingly, the point source assumption shows a similar performance to the finite fault assumption as long as the period range is longer than 4 s. Another alternative is to convolve the source time function of the large earthquake with the Green's functions retrieved with a station located close to the earthquake source. We validate this approach by simulating the long-period ground motions ($T > 4$ s) of the 2007 Chuetsu-oki earthquake. Up to now, these techniques have only been applied to crustal earthquakes. With the recent increase of offshore continuous observation systems, such as the S-net, DONET, and JMA networks, the application can be extended to subduction earthquakes with finite source modeling using offshore-onshore Green's functions. The ambient seismic field has a potential to overcome the current limitation of velocity structure modeling, especially for shallow oceanic soft layers. However, some issues still need to be solved, such as the Green's function amplitude calibration, the earthquake depth limitation, the period range limitation, potential azimuthal variations, and seasonal variation.

Keywords: seismic interferometry, finite fault, ground motion simulation

©2017. Japan Geoscience Union. All Right Reserved. 

# Dynamic Rupture Simulation of Near Fault Ground Motions for Surface and Buried Faults: Comparison of Dip Slip and Strike Slip Faults

*Kenichi Kato[1], Yasuhiro Ohtsuka[1], Monika Tadokoro[1], Tetsushi Watanabe[1], Tomiichi Uetake[2], Kazuhito Hikima[2]

1. Kobori Research Complex Inc., 2. Tokyo Electric Power Company Holdings, Inc,

From the view point of earthquake engineering, it is interesting topics which fault types, surface faults or buried faults, generate stronger ground motions. Somerville (BSSA 2003) and Kagawa et al. (EPS 2004) indicate from observed records in near faults region that ground motions from the buried faults show larger response spectra than those from the surface faults, in particular at high frequency range. Since the observational findings were derived from the restricted number of data, Dalguer et al. (BSSA 2008) and Pitarka et al. (BSSA 2009) conducted dynamic rupture simulation of near fault ground motions for strike slip events at many points on the surface. They conclude that the buried faults show larger amplitude than that of the surface faults, consisting to the observational findings by Somerville (2003) and Kagawa et al. (2004).

Because the target of these studies is strike slip events, Kato et al. (SSJ autumn meeting, 2016) carried out dynamic rupture simulation for reverse faults. They indicate that the surface faults show larger amplitude than the buried faults at near fault region with shortest distance from the fault plane, Xsh, shorter than 2km. This is the opposite relation obtained from strike slip events by Dalguer et al. (2008) and Pitarka et al. (2009), but they do not deal with such the short distance. Since near fault strong motion is remained to be solved, we carried out dynamic rupture simulations for strike slip events assuming the consistent fault parameters for dip slip events by Kato et al. (2016). We compare near fault strong motions for the strike slip events between buried and surface faults, and also compare to those from dip slip events.

Fault plane with 20 km length and 20 km width with dip angle of 90 degree is embedded in the homogeneous half space. Rupture initiation depth, H, for the surface fault model (SFM) is 7.5 km, and the stress drop is assumed to be 5 MPa. Two types of H, 7.5 km and 10.0 km, are set to the buried fault model (BFM), and the stress drop is assumed to be 7.5 MPa, which is higher than that of SFM. The stress drop shallower than 3 km is set to be depth dependent; 5 MPa to 0 MPa or -2.5 MPa for the SFM and 7.5 MPa to -20MPa for the BFM. We applied 3D-FDM with slip weakening law for the simulation (Kase and Kuge, GJI 2001).

From the spontaneous rupture, we obtained the moment magnitude, Mw, 6.9 from the SFM, and Mw 6.8 for the BFM. The peak ground velocity (PGV) of fault parallel component, FP, with Xsh shorter than 2km from the SFM show larger amplitude than that of the BFM due to the effects of fling step indicated by Hisada and Bielak (BSSA 2003). On the other hand, the PGV of fault normal component, FN, from the BFM show larger amplitude than that of the SFM due to the combined effect of large stress drop and rupture directivity.

Relatively large PGV of dip slip events are obtained at the foot wall side for FN, and the hanging wall side for vertical component with Xsh shorter than 2 km (Kato, 2016). When we compare the above PGV, the SFM show larger amplitude than that of BFM.

Summarizing the results of strike and dip slip events for the near fault region with Xsh shorter than 2 km

©2017. Japan Geoscience Union. All Right Reserved. 

from spontaneous rupture simulation, the PGV from the SFM show larger amplitude than that of the BFM, except for FN component of strike slip events. The strong ground motions in near fault region depend largely on the assumption of fault parameter at shallow depth. Note that the PGV from BFM show larger amplitude than that of the SFM at the region with Xsh longer than 2 km. We will further investigate the modeling of surface and buried fault, constraining the observed findings.

We acknowledge to Dr. Kase and Dr. Nagano with fruitful discussion.

Keywords: Dynamic Rupture Simulation, Surface Fault, Buried Fault, Near Fault, Ground Motions

©2017. Japan Geoscience Union. All Right Reserved. 

# Characteristics of Near-Fault Ground Motions during the 2016 Kumamoto, Japan, Mainshock

*Tomotaka Iwata[1], Kimiyuki Asano[1]

1. Disaster Prevention Research Institute, Kyoto University

During the mainshock of the 2016 Kumamoto earthquake, which caused the surface rupture, strong motions (JMA seismic intensity of 7) at Mashiki town and Nishihara village were observed near the surface rupture. We carefully integrated the observed acceleration records to velocities and displacements with correcting the base-line change in acceleration records, which would be caused by the effect of tilting of the seismometer. The corrected observations show large permanent displacements, which include near-fault terms. The amounts of permanent displacements coincide to geodetic observation results. We discuss those ground motion characteristics and compare those with other near-fault ground motion records.

Keywords: Near-source ground motions, The 2016 Kumamoto earthquake

©2017. Japan Geoscience Union. All Right Reserved. 

# A simplified source model to explain damaging near-source ground motions during the 2016 Kumamoto earthquake

*Atsushi Nozu[1], Yosuke Nagasaka[1]

1. Port and Airport Research Institute

A simplified source model was developed for the main shock of the 2016 Kumamoto earthquake (April 16, 2016, 1:25 JST, $M_J$7.3) for the purpose of estimating strong ground motions at the sites of significant damage. The first priority was to reproduce strong ground motions in the region extending from Mashiki Town to Minami-Aso Village where significant damage to highway bridges was found. Corrected EGF method (Kowada et al., 1998; Nozu and Sugano, 2008; Nozu et al., 2009) was used for the simulation. Details of the source model and the simulation can be found at http://www.pari.go.jp/bsh/jbn-kzo/jbn-bsi/taisin/sourcemodel/somodel_2016kumamoto.html. The digital data of the source model can also be found at the same website.
The near-source region of the earthquake is shown in the top-right panel of the figure. The rectangle in the map indicates the surface projection of the fault plane (length:40 km; width:20 km; strike=232 degrees; dip=84 degrees) that was used for the waveform inversion (Nozu and Nagasaka, 2017). According to the waveform inversion (bottom-right panel of the figure), a region of significantly large slip and slip velocity (hereafter referred to as “Asperity 3” in this article) existed around 15 km northeast of the hypocenter (indicated by a star). In Mashiki Town (KMMH16), a large-amplitude pulse-like ground motion with a predominant period of 1 s was observed, which resulted in significant damage. However, if we consider the fact that Mashiki Town is located between the hypocenter and Asperity 3, the damaging ground motions in Mashiki Town cannot be attributed to the rupture of Asperity 3. On the other hand, in the region northeast of Mashiki Town, the effect of the rupture of Asperity 3 should have been predominant. Thus, the near-source strong ground motions could have been dependent on the relative locations of the site and the asperities.
Site amplification factors evaluated in a conventional study (Nozu and Nagao, 2005) was used except for two stations. At KMM006, a newly evaluated site amplification factor (http://www.pari.go.jp/bsh/jbn-kzo/jbn-bsi/taisin/research_jpn/research_jpn_2016/jr_48.html) was used, because the site was relocated after the evaluation of the conventional site amplification factors. At KMMH16, a newly evaluated site amplification factor was used to include recently obtained data. However, the site amplification factors at these sites did not differ significantly from the old ones. At Komori, Nishihara Village and Kawayo, Minami-Aso Village, the site amplification factors were evaluated based on weak motion records obtained by Osaka University. The phase characteristics of the Green’s functions were evaluated using weak motion records that occurred in the source region.
The simplified source model is shown in the bottom-right panel of the figure. Three asperities were modeled referring to the results of waveform inversion, namely, Asperity 1 and Asperity 2 at approximately 5 km northeast of the hypocenter and Asperity 3 at approximately 15 km northeast of the hypocenter. The rupture of each asperity was assumed to start from the individual rupture staring point indicated by the open star and to propagate radially. The rise time of each asperity was determined based on the relation by Kataoka et al. (2003) except for the Asperity 3, for which a slightly larger rise time was assigned to reproduce observed ground motions at Komori, Nishihara Village. The Q value for the region proposed by Katoh (2001) ($Q=104\ f^{0.63}$) was used. Multiple nonlinear effects were considered in the simulation (Nozu and Morikawa, 2003; Nozu and Sugano, 2008). Among the two parameters to consider the multiple nonlinear effects, $\nu_1$ was determined based on the ratio of peak frequencies between the strong and weak motion records. $\nu_2$ was determined to appropriately reproduce the amplitude of the later phases.

©2017. Japan Geoscience Union. All Right Reserved. 

The left panel of the figure compares the observed and synthetic velocity waveforms. The main features of the velocity waveforms including the large-amplitude pulse at KMMH16 were successfully reproduced. The Fourier spectra at near-source stations were also successfully reproduced.

Acknowledgment: Ground motions records were provided by the National Research Institute for Earth Science and Disaster Resilience, the Kumamoto Prefectural Government, the Japan Meteorological Agency and Dr. Yoshiya Hata of Osaka University.

Keywords: The 2016 Kumamoto earthquake, strong ground motion, source model, Corrested EGF method, site amplification factor

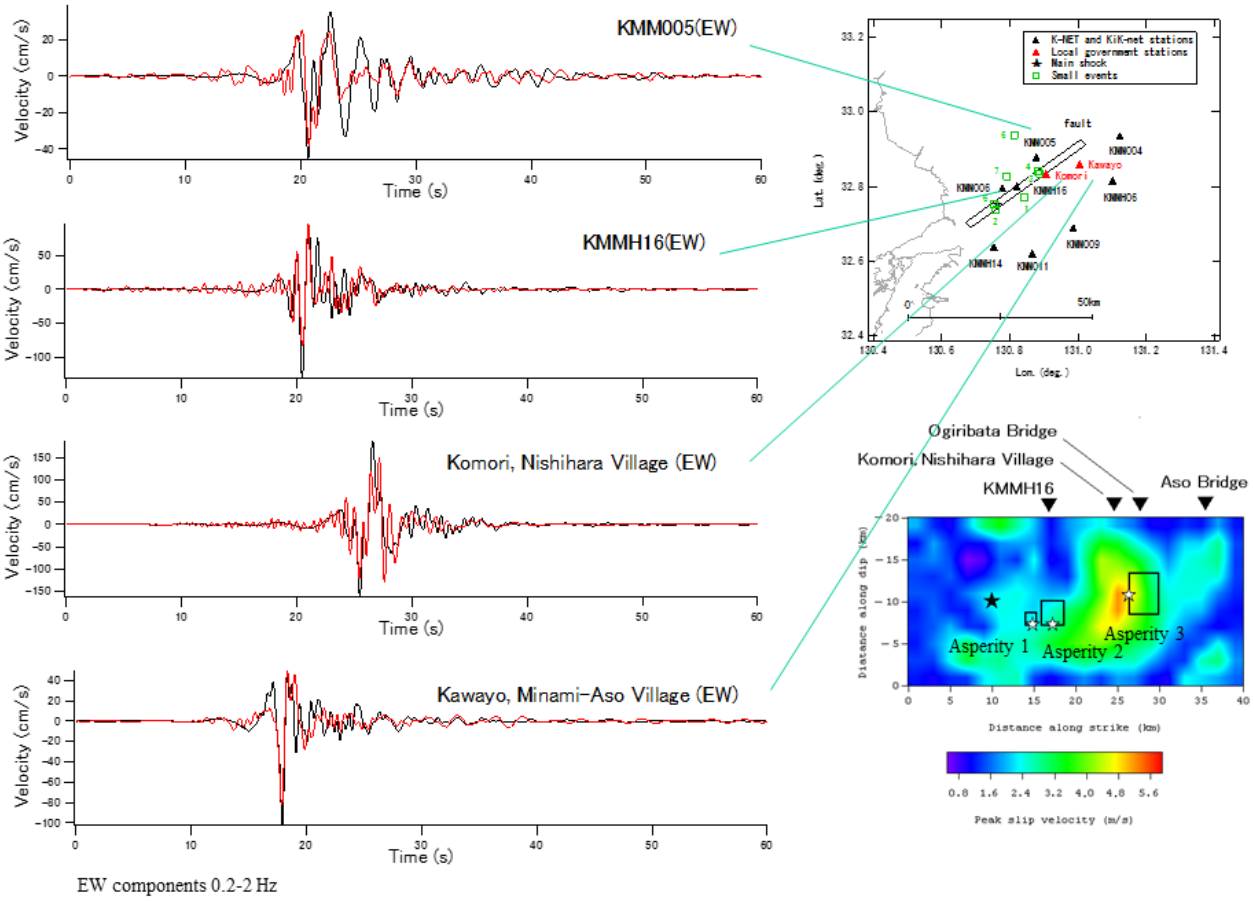


©2017. Japan Geoscience Union. All Right Reserved. 

# Influence of Surface Rupturing and Shallow Subsurface Structure on Near-Fault Pulse-Type Motions during the 2016 Kumamoto Earthquake

*Masayuki Nagano[1], Kazuhito Hikima[2]

1. Tokyo University of Science, 2. Tokyo Electric Power Company

INTRODUCTION

The 2016 Kumamoto earthquake with MJ7.3 occurred in the midnight of April 16th (hereafter referred as the main shock) and massive shaking with the JMA intensity of 7 hit to densely populated area of Mashiki-machi leading to devastating damages to lots of wooden houses. Features of near-fault ground motions recorded in Mashiki-machi are summarized as follows: (1) Pulse-type motions with predominant period of 1 s. were recorded adjacent to surface rupturing. (2) Amplitude level was larger than the Takatori motion during the 1995 Kobe earthquake. (3) Principal axis was close to east-northeast direction parallel to Futagawa segment. (4) Spatial variation of recorded ground motions is large in short distance within 1 km.

Discussion has been made for why the pulse-type near-fault ground motions with large amplitude were generated, e.g., rupturing in deep and shallow part of seismic fault, site amplification in shallow and deep part of subsurface structure. Quantitative evaluation of amplification mechanism of pulse-type near-fault ground motions is important for predicting input ground motions to structures adjacent to seismic faults. In this study, strong ground motions in Mashiki-Machi are theoretically synthesized using the finite source model by Hikima (2016) based on waveform source inversion analyses. Then, amplification mechanism is discussed based on numerical approach focusing on effects of rupturing in deep and shallow part of seismic fault and the shallow and deep part of subsurface structure.

METHODOLOGY

The thin layer method (TLM) is used as a theoretical evaluation method of ground motions. The TLM is thoroughly verified in the "Benchmark Test Project" in Japan (Hisada et al., 2012), as a practical and theoretical method for ground motion evaluation in the horizontally flat strata. Velocity structure in Mashiki-Machi is referred from the PS logging data at the KiK-net Mashiki site for the shallow part and the "preliminary nationwide velocity structure model" for the deep part. Source process evaluated by Hikima (2016) has two segments for the Futagawa faults stretched from the Hinagu faults. Although the finite source model deals with frequency range from 0.05 to 0.8 Hz, ground motions are calculated in the frequency range up to 2 Hz considering importance of frequency component around 1 s. in observed pulse-type ground motions from the engineering's point of view.

EFFECT OF SURFACE RUPTURING AND SUBSURFACE STRUCTURES ON GROUND MOTION AMPLIFICATION

Observed ground motions at the KMMH16 site during the main shock were simulated by the TLM. Theoretically synthesized ground motions fairly reproduced the observed ones. Frequency component around 1 s.is rather underestimated, partly because the finite source model do not guarantee the higher frequency component over 0.8Hz.

Effects of surface rupturing on ground motion amplification are discussed. Theoretical ground motions are calculated for hypothetical source models deleting the sub-fault row in the shallow part of finite source model. Peak ground velocities become small especially in longer period range than 2 s when shallow

©2017. Japan Geoscience Union. All Right Reserved. 

sub-fault area is ignored.
Next, ground motions are evaluated focusing on effects of subsurface structures on amplification characteristics by replacing low velocity strata to the profile of the seismic bedrock. In ground motions in the bedrock model, the predominant period component around 1 s. diminished despite that variation of peak ground velocities is small.

Keywords: The 2016 Kumamoto earthquake, Near-Fault, Pulse-Type Motions

©2017. Japan Geoscience Union. All Right Reserved. 

# The ground motion characteristics along a north-south line in the Kumamoto Plain, using earthquake and array microtremor observation data

*Masahiro Korenaga[1], Seiji Tsuno[1], Kyosuke Okamoto[1], Kosuke Chimoto[2], Hiroaki Yamanaka[2], Nobuyuki Yamada[3], Takeshi Matsushima[4]

1. Railway Technical Research Institute, 2. Tokyo Institute of Technology, 3. Fukuoka University of Education, 4. Institute of Seismology and Volcanology, Faculty of Science, Kyushu University

In order to evaluate the ground motion characteristics in the Kumamoto plain, we are observing earthquakes on the north-south line in the Kumamoto Plain, right after the 2016 Kumamoto earthquake. We calculated ground amplification characteristics at each site using the aftershock observation data of the 2016 Kumamoto Earthquake, and estimated the S-wave velocity structures by array microtremor observation data around the seismic stations.

We installed 15 temporary seismic stations at intervals of 300m to 2.5km along a north-south line in the Kumamoto Plain, a section of 15km from the outer rim of Mt. Kinbo (northern end of the Kumamoto plain) to the Uto Peninsula (southern end). We obtained seismic data of the main shock (Mj 7.3) on 16th April, 2016 at 2 sites, northern part of a north-south line in the Kumamoto Plain. We evaluated site amplifications for temporary seismic sites to reference sites, using the seismic wave data by earthquake events occurred around Mt. Aso. Reference sites are permanent seismic station (KU.KMP1) in the outer rim of Mt. Kinbo installed by Institute of Seismology and Volcanology, Faculty of Science, Kyushu University, and temporary rock site in Uto Peninsula. We calculated the Fourier spectra for a time-window of 5 seconds after initial S-wave arrival, and the Fourier spectra with the Parzen window of 0.4Hz at temporary stations in the sediment sites were divided by that at the reference site. Site amplifications at the survey line middle and southern part sites installed in the alluvial lowland have a factor of dominantly larger than 1 in the frequency 1-2 Hz, but the amplification factor and the characteristics in the frequency above 3 Hz showed a difference for each site. At several sites close to the northern end of the survey line, the peak of the frequency is higher (2-5 Hz) than the sites in the alluvial lowland, and the amplification factor is smaller. It suggests that the surface ground structure changes complicatedly along a north-south line in the Kumamoto Plain. In addition, we confirmed that the characteristics of the NS and EW component of the spectral ratio between the northern sites of the survey line and KU.KMP1 are clearly different around 1-3 Hz. It is assumed that there is some seismic anisotropy, but we will further investigate its cause.

And also, we performed array microtremors observations at the seismic stations, to estimate the local site effects along a north-south line in the Kumamoto Plain. We installed vertically accelerometer in a double triangle with an edge length of 1.5m to 24m and its center, and measured at a sampling frequency of 100Hz for 10 to 20 minutes. We obtained phase velocities of Rayleigh waves by the SPAC method, estimated S-wave velocity structures through inversion analysis of dispersion curves with genetic algorism (GA). We confirmed tentatively that the low velocity layer was deposited on the surface at sites in the alluvial lowland and its thickness might be 15m or more. We will discuss the ground motion characteristics along a north-south line in the Kumamoto Plain, using the site amplifications estimated by seismic observation data and S-wave velocity structures estimated by array microtremor observation data.

Keywords: Ground motion characteristics, 2016 Kumamoto earthquake, North-south line in the Kumamoto Plain

©2017. Japan Geoscience Union. All Right Reserved. 

©2017. Japan Geoscience Union. All Right Reserved. 

# Dense Microtremor observations in disaster area due to the 2016 Kumamoto Earthquake

Takao Kagawa[1], *Shohei Yoshida[1], Hiroshi Ueno[1]

1. Tottori University Graduate School of Engineering

Microtremor observations were conducted in Mashiki town and Minami-Aso village where severe damages spread over due to the 2016 Kumamoto Earthquake. Two targets are set for the observations. One is searching out the difference of ground motion between surface faulting areas without severe damage and severely damaged areas without surface faulting. Another is assessing the effect of surface geology and geographic transition on spotted damage distribution in downtown area. For the purposes, 3 components single station observations are conducted to detect predominant period at the site and array observations are made for evaluating surface velocity structures. Using the records fro microtremor observations and previously conducted aftershock observations, productive discussions about causes of disaster are expected.

Keywords: The 2016 Kumamoto Earthquake, Mashiki town, Minami-Aso village, Microtremor observation

©2017. Japan Geoscience Union. All Right Reserved. 

# Characterized source model for estimating strong ground motions during one of the largest foreshocks (Mw 6.0) of the 2016 Kumamoto Earthquake

*Susumu Kurahashi[1], Ken Miyakoshi[2], Kojiro Irikura[1]

1. Aichi Institute of Technology, 2. Geo-Research Institute

1. Introduction
One of the largest foreshocks (Mw 6.0) of the 2016 Kumamoto earthquake occurred along the Hinagu fault zone in Kyushu, Japan, on April 15, 2016. The maximum seismic intensity with 6 lower was observed at KMMH16 (Mashiki, epicentral distance: 11km) and KMMH14 (Toyono, epicentral distance: 8km) station. PGA of 557.9 gal is observed at the KMMH14. We estimated the characterized source model based on the slip distribution results of the waveform inversion using the strong motion data and the empirical Green's function method.
2. Source model inferred from the waveform inversion results
We analyzed the slip distribution during this earthquake using the multi-time window linear waveform inversion method (Sekiguchi et al., 2000). The data sets used for the inversion analysis were velocity waveforms of S-waves parts in the frequency range 0.1-1.0Hz at 11 stations (KiK-net, K-NET). The Green's functions were calculated using the one-dimensional velocity structure models by the discrete wavenumber method (Bouchon, 1981) with the reflection and transmission matrix method (Kennett and Kerry, 1979) at the stations. A fault plane was assumed referring to the aftershock distribution and the moment tensor solution determined by F-net.
The fault plane is divided into 81 subfaults of 1.5km×1.5km. The temporal moment release history from each subfault is modeled by a series of 4 smoothed-ramp-functions with a rise time of 0.8 second each separated by 0.4 second.
Large slip area is constructed in the proximity of the hypocenter.Seismic moment and rupture velocity are estimated 1.6×1018Nm, 2.7km/s, respectively. The synthetic waveforms at KMMH14 station fit the observed ones reasonably.

3. Characterized source model inferred from the waveform inversion results
The characterized source model is constructed based on the slip distribution from the waveform inversion. We extracted asperity from the slip distribution and high rate area (HRA) from the moment rate distribution by the criterion of Somerville et al. (1999). The area and location of the asperity and the HRA are estimated to be almost the same.
4. Estimation of strong motion generation area (SMGA) using empirical Green's function method
We analyzed the SMGA model using the empirical Green's function method. In particular, we attempted to simulate the strong ground motions at KMMH14 located near the source fault. As a result, the location of the SMGA is nearly the same as the estimated large slip area from the waveform inversion results. We obtained one of the best-fitting SMGA models choosing the starting point, rupture velocity, and rise time by comparing simulated and observed ground motions including the ground motions at KMMH14. The SMGA area and stress parameter are calculated about 33 $km^2$ and 7.5 MPa, respectively. The scaling relationship SMGA area versus seismic moment is consistent with on the scaling law of combined of asperities versus seismic moment by the previous study (Irikura and Miyake, 2001).
5. Conclusion
We estimated the characterized source model of the Mw 6.0 forshock of the 2016 Kumamoto earthquake

©2017. Japan Geoscience Union. All Right Reserved. 

based on the slip distribution results of the waveform inversion using the strong motion data and the empirical Green’ s function method. The asperity, the HRA and the SMGA of this earthquake are collocated with nearly the same area.

Acknowledgements. Seismic waveform data of the K-NET and KiK-net were used. This study was based on the 2016 research project 'Improvement for uncertainty of strong ground motion prediction' by NRA (Nuclear Regulation Authority).

Keywords: Foreshock of the 2016 Kumamoto earthquake, strong ground motion, characterized source model

©2017. Japan Geoscience Union. All Right Reserved. 

# Strong ground motion simulation of the main shock of the 2016 Kumamoto Earthquake using the pseudo point-source model and its improvement

*Yosuke Nagasaka[1], Atsushi Nozu[1]

1. Port and Airport Research Institute

Many near-fault strong motion records were obtained during the main shock of the Kumamoto, Japan, earthquake on April 16th, 2016. In general, observed records of such a large earthquake reflect the finiteness of the fault, that is, directivity effect. On the other hand, strong motion simulations using simple point sources and empirical site amplification and phase characteristics have well reproduced observed strong motions of large earthquakes such as the 1995 Kobe and 2011 Tohoku Great earthquakes (for example, Nozu, 2016). Investigating the applicability of the point source model to large earthquakes is important to understand the mechanism of strong motion generation. In this study, then, we constructed a pseudo point-source model (Nozu, 2012) for the main shock of the Kumamoto earthquake and the simulation results were compared with the observed records.
In the pseudo point-source model, the source spectrum is combined with the path effect, empirical site amplification factors, and empirical phase characteristics from small earthquakes to synthesize strong motions. Source parameters include the location of the point sources, corner frequencies, and seismic moments. In our model for the main shock of the 2016 Kumamoto earthquake, three subevents were placed on the fault plane along Futagawa fault: two of them were placed below Mashiki Town, about 5 km northeast from the epicenter, and the other was placed below Nishihara Village, about 15 km northeast from the epicenter. Two subevents were placed around Mashiki town to reproduce the characteristic velocity pulses and the trough in the observed Fourier spectrum at Mashiki, which was considered due to the interference of the seismic waves from two different sources. The observed and synthetic velocity waveforms (0.2-2Hz) and acceleration Fourier spectra were compared. The synthetic results generally reproduced the main features of the observed records, however, discrepancies were also observed. One of them is the underestimation in the frequency range below 0.6 Hz, which was considered due to the contribution from shallow slip including near-field and intermediate-field terms, because the effect of shallow slip were not considered in the point source models. Large permanent displacements could be due to the near-field and intermediate-field terms. We need to incorporate the effect of shallow slip including these terms if they contribute to near-fault ground motions around 0.6 Hz, because ground motions in this frequency range contribute to damage to structures. Another discrepancy found in the point-source model is the underestimation at the stations northeast of the epicenter, around Aso Caldera. This is presumably due to the fact that the point source models cannot capture the directivity effect, whereas the actual rupture proceeded northeast and caused significant forward directivity effect at stations located northeast of the fault.
We need to model not only the deep subevents but also the shallow slip in order to adequately conduct strong motion simulation for the 2016 Kumamoto earthquake. We will use an ordinary point source model for the deeper part, and incorporate the effect of shallow slip including near and intermediate-field terms. The original model was intended to explain whole strong motions without considering the shallow slip. In the new model, by incorporating the effect of the shallow slip, the parameters for the deeper point source will also be affected. The new model will be presented in the meeting.

©2017. Japan Geoscience Union. All Right Reserved. 

Keywords: The 2016 Kumamoto earthquake, strong ground motion simulation, pseudo point-source model

©2017. Japan Geoscience Union. All Right Reserved. 

# Estimation of characterized source model of the mainshock in the 2016 Kumamoto earthquakes using the stochastic Green's function method

*Atsuko Oana[1], Kazuo Dan[2], Junichi Miyakoshi[2], Hiroyuki Fujiwara[3], Nobuyuki Morikawa[3], Takahiro Maeda[3]

1. Shimizu Corporation, 2. Ohsaki Research Institute, 3. National Research Institute for Earth Science and Disaster Resilience

We estimated a characterized source model for the mainshock in the 2016 Kumamoto earthquakes using the stochastic Green's function method, in preparation for strong motion prediction at points where no observation records were obtained.
Records of the seven KiK-net observation stations, including KMMH16 (Mashiki), were targets of this study. First, the strong motions on the engineering bedrock were estimated in order to remove the site effects of the shallow soil from the observation records. In concrete, the soil models were identified so that the transfer functions between the surface records and the borehole records could be reproduced for less 5 Hz. Then, the strong motions on the engineering bedrock were calculated by the multiple reflection theory using the identified soil models and the borehole records. The NS and EW components were calculated separately, because it was difficult to invert both of them back to the motions on the engineering bedrock using the common identical soil model.
Next, one-dimensional velocity structure models from the seismic bedrock to the engineering bedrock were assumed based on the Japan integrated velocity structure model (Koketsu et al., 2012), then those models were adjusted so that the dominant frequencies of the models corresponded to those of the H/V spectral ratios of the small aftershock records.
The stochastic Green's functions were generated using the stochastic amplitude model and the envelope function model (Boore, 1983), especially for the area close to the fault. Then, the waves that had bell-shape forms were selected based on Kagawa (2004). The cutoff frequency $f_{max}$ was assumed to be 4 Hz. The Q-value was $62f^{0.87}$ (for $f$ less than 1 Hz) taken from Satoh (2016). The source model was assumed as an SMGA (Strong Motion Generation Areas) model. The location and area of SMGA were set by trial and error, inside the region of the source inversion of Asano and Iwata (2016). The slip of each SMGA was determined with reference to the slip distribution of source inversion (e.g., Asano and Iwata, 2016; Hikima, 2016), and at the same time, so that the displacements and the velocity response spectra in long period range of our simulation agreed with the observed ones. The stress drop of each SMGA was determined so that the accelerations, velocities, and velocity response spectra in short period range of our simulation agreed with the observed ones. The location of the rupture initiation point of Hinagu fault was the same as that by JMA (2016), and that of Futagawa fault was slightly deeper than Hinagu one and located at the southern edge of the fault. The rupture velocity of the small SMGA in Futagawa fault was 2.7 km/s, and that of the large SMGA in Futagawa fault and that of Hinagu fault were 3 km/s.
The obtained source model had a short-period level of $1.14\times10^{19}$ Nm/s$^2$, which was smaller than Satoh (2016) and Irikura et al. (2017) and larger than Nakano and Kawase (2016). Furthermore, the short-period level was smaller than the empirical relationship between the seismic moment and short-period level of crustal earthquakes proposed by Dan et al. (2001), and was slightly smaller than the empirical relationship of crustal earthquakes caused by strike-slip faults proposed by Dan et al. (2011). The averaged response spectral ratio between the observation records and the simulation results became almost 1 in the period range of 0.2-5 s. However, the ratio was smaller than 1 in the period range longer

©2017. Japan Geoscience Union. All Right Reserved. 

than 5 s. This is because the seismic moment of the obtained SMGA model was about 60 % of that of the whole fault (e.g., F-net, 2016). While the duration of simulation results in the area close to the fault trace corresponded well to the observed ones, those of the simulation results in the area far from the fault trace were shorter than the observed ones. This attributes to a problem for setting the amplitude and the envelope function of the Green's function in the area far from the fault trace.

Keywords: 2016 Kumamoto earthquake, Stochastic Green's function method, Characterized source model

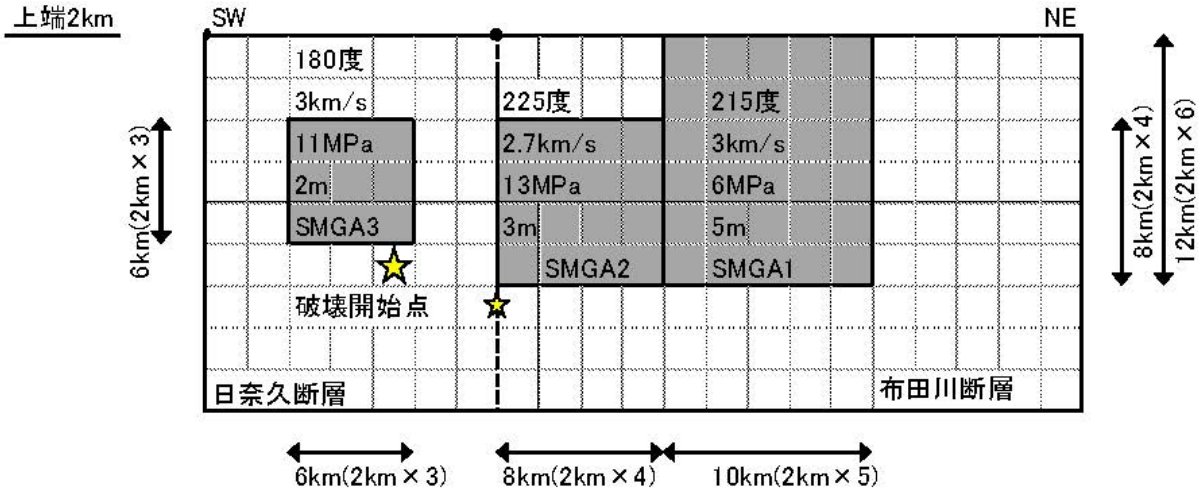


（数値：すべり角[度]、破壊伝播速度[km/s]、応力降下量[MPa]、すべり量[m]）

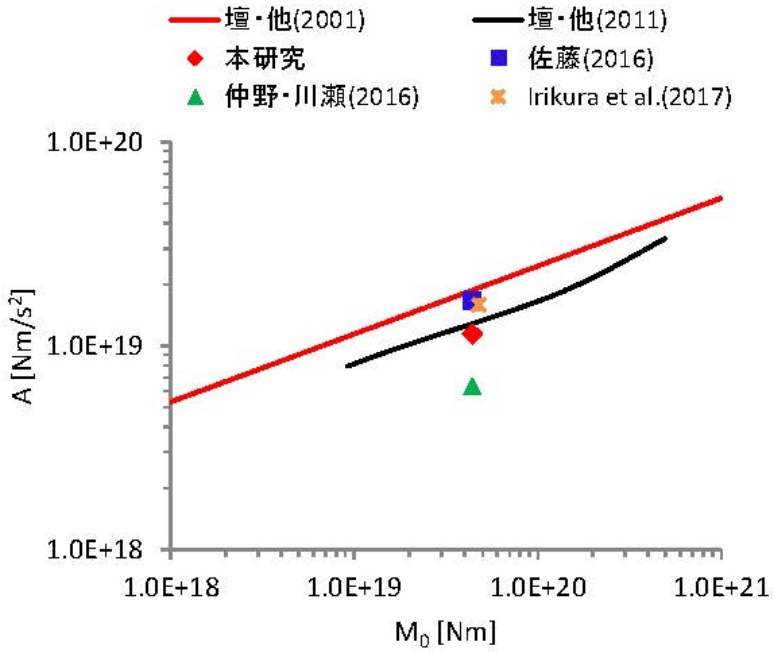


※本研究、佐藤(2016)、仲野・川瀬(2016)の地震モーメント $M_0$ は F-net の $4.42 \times 10^{19}$ Nm とした。佐藤(2016)と Irikura et al.(2017)の短周期レベル A は、SMGA の応力降下量と面積を用いて算出した。

©2017. Japan Geoscience Union. All Right Reserved. 

# Source model and strong ground motion simulation for the 2016 Mid Tottori prefecture, Japan, earthquake ($M_w$6.2) based on the empirical Green's function method

*Kazuhiro Somei[1], Takaaki Ikeda[2], Toshimitsu Nishimura[1], Ken Miyakoshi[1]

1. Geo-Research Institute, 2. Nagaoka University of Technology

At 14:07 Japan Standard Time (JST=UT+9) on October 21, 2016, an inland crustal earthquake ($M_{JMA}$6.6, $M_w$6.2) with strike-slip occurred in the mid Tottori prefecture, Japan. Strong ground motions with a peak acceleration 1381 cm/s$^2$ were recorded at one of the nearest strong motion stations, TTR005, about 10 km away from the hypocenter. For understanding the physical mechanisms of strong motion generation processes during this event, we estimate the source model composed of strong motion generation areas (SMGA) to explain the observed strong motion records in broadband frequency range between 0.3 and 10 Hz.

In this study, we use the empirical Green's function method to simulate the broadband strong motion records at 18 sites of K-NET and KiK-net located around the source region. The observed ground motion records of $M_w$4.1 event (element event) occurring at 12:12 on October 21, 2016, are used as the empirical Green's functions. For an objective estimation of corner frequencies for the target and element events, we apply the source spectral ratio fitting method (Miyake et al., 1999). From the obtained corner frequencies, scaling parameters $N$ and $C$, which required for the empirical Green's function method of Irikura (1986), are determined. Then, the parameters of each SMGA (e.g., the size, rupture starting point, rise time, rupture velocity, and relative location from the hypocenter) are estimated by trial and error method. Since we can clearly see the S-wave portion consists mainly of two wave packets for observed waveform at TTR005, we assume two squared SMGAs on the fault plane, and will call the SMGA that generates the first S-wave packet SMGA1 and that generating the second SMGA2.

As a result, we construct the source model with SMGA1 located including the hypocenter and SMGA2 located north from the hypocenter. The sizes of SMGA1 and 2 are 30.3 and 19.4 km$^2$, respectively. The stress drops of both SMGAs are estimated to be same as 16.6 MPa. Rupture propagations within SMGAs bring forward and backward rupture directivity effect in ground motion observed at TTR005 that is located near-source fault: The forward directivity effect by SMGA1 contributes to the pulse-shape wave packet for fault-normal component observed at TTR005. On the other hand, the random-shape wave packet is generated by the backward directivity effect from SMGA2. However, the amplitude of pulse-shape wave from SMGA1 is not as large as that expected from the ground motion prediction equation (GMPE), because the rupture within SMGA1 propagates bilaterally from the center of SMGA1 to both north and south directions. For other sites located around the source region, the SMGA1 mainly reproduces the observed acceleration, velocity, and displacement waveforms fairly well. Thus, the near-source strong ground motion observed at TTR005 gives us the insight into the possiblity for the presence of SMGA2. In order to improve the reproducibility of observed ground motions, the parameters of SMGAs need to be examined objectively in more detail.

Acknowledgements: We use the hypocentral information catalog of JMA, the moment tensor catalog by F-net, and the strong motion data from K-NET, KiK-net, and F-net provided by NIED.

Keywords: The 2016 Mid Tottori prefecture earthquake, Strong motion generation area, Empirical Green's function method

©2017. Japan Geoscience Union. All Right Reserved. 

©2017. Japan Geoscience Union. All Right Reserved. 

# A heterogeneous SMGA model for plate boundary earthquakes

*Haruko Sekiguchi[1], Kimiyuki Asano[1], Tomotaka Iwata[1]

1. DPRI, Kyoto University

Seismic waves in the frequency range 0.1–10 Hz are mainly radiated from strong motion generation areas on a source fault. A heterogeneous SMGA (Strong Motion Generation Area) model was constructed inspired by the area-stress drop relationship of SMGAs of plate boundary earthquakes. The relationship shows large scatter of average stress drop for small SMGAs and small scatter for large SMGAs. The relationship was well modeled by adopting $k^{-1}$ spatial spectrum and lognormal probability distribution for the stress drop distribution, and tuning the parameters of those distributions. This model may make it possible to predict the strong short-period pulse amongst the SMGA pulse, which has been indicated by forward waveform modeling in previous studies (e.g., Matsushima and Kawase, 2006; Nozu 2012; Kurahashi and Irikura, 2013).

Keywords: Strong motion generation area, heterogenous source, stress drop

©2017. Japan Geoscience Union. All Right Reserved. 

# Parameter Study on Near Fault Strong Ground Motion Considering Randomness of Faulting Process

*Junpei Kaneda[1], Yoshiaki Hisada[1]

1. Kogakuin University

During the 2016 Kumamoto earthquake, the near fault strong ground motions in Mashiki City showed that the EW components (closet to the fault normal direction) were dominant over the NS components. This was probably caused by the combined effects of the upward directivity pulse (e.g., Miyatake (2016)) and the fling step (e.g., Hisada et.al. (2016)). On the other hand, the near fault strong ground motion in Nishihara Village also showed the dominant EW components, which was caused by the fling step, but did not showed the forward directivity pulse. This may be caused by the complex faulting process, and/or the complex underground structures, which prevents the generation of directivity pulses (e.g., Hisada et.al. (2016)). In order to confirm these phenomena, we carried out the parameter studies based on the recipe for strong motion prediction method. We will present the detail results on the conference.

Keywords: Near Fault Strong Ground Motion, Directivity Pulse, Randomness of Faulting Process

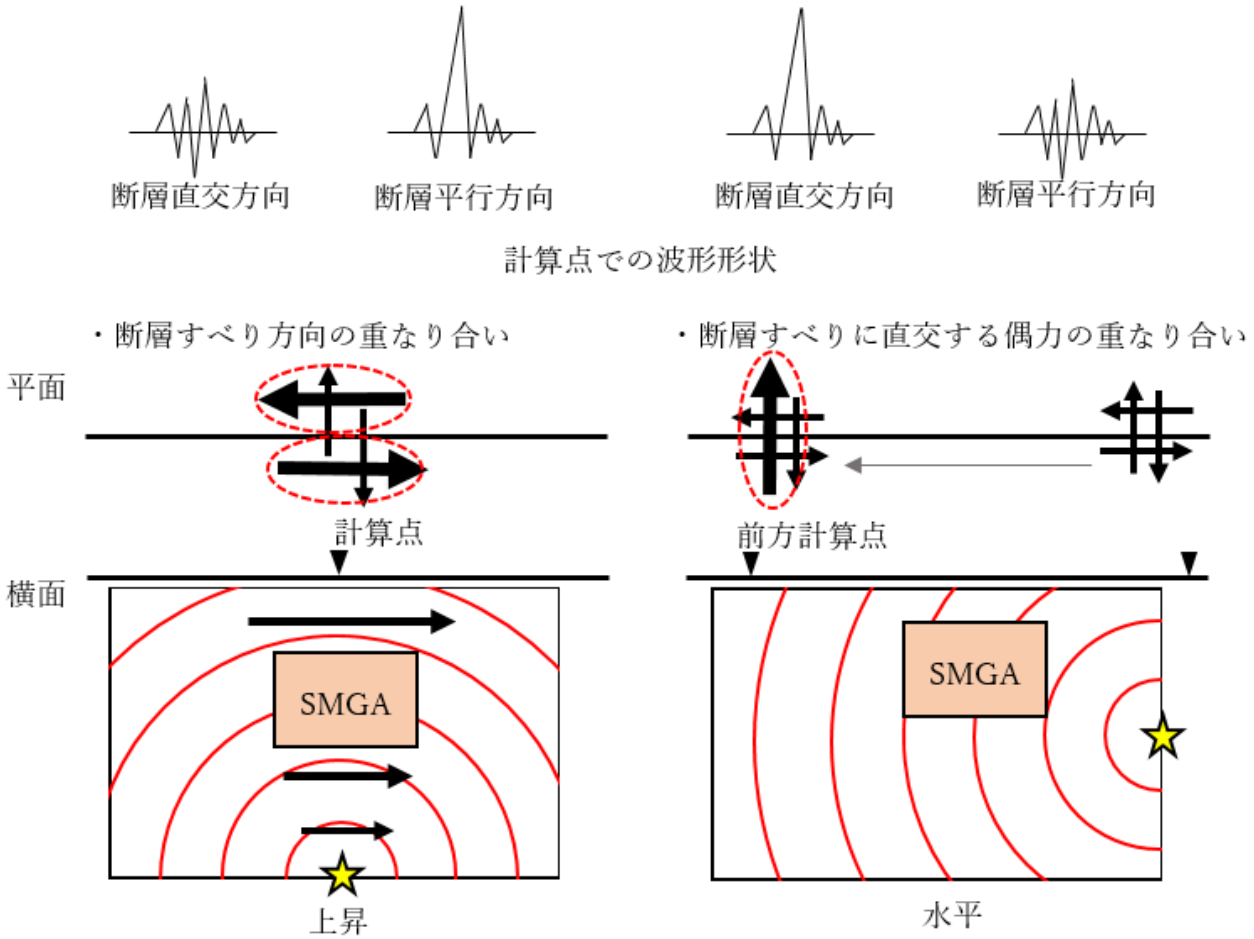


図 1 伝播特性と指向性パルス発生の概念図(宮武(2016)を参照)

©2017. Japan Geoscience Union. All Right Reserved. 

# Site response of vertical component ground motion excited by obliquely incident S wave

*Kunikazu Yoshida[1], Ken Miyakoshi[1]

1. Geo-Research Institute

We investigate vertical ground motion of S-wave portion in a continuous velocity structure model. In many case, vertical ground motions of S-wave part have been assumed as a wavefield of that part is dominated by P wave. However, this assumption sometimes seems to be inappropriate to real data. We calculated spectral ratios of surface to borehole ground motions on P and S wave parts recorded at 6 KiK-net vertical array sites. At some sites (e.g., KMMH16), the spectral ratios on P and S wave parts have similar shapes, however, some other sites (e.g., TYMH02) indicated different shapes of spectral ratio between P and S wave parts. The site which have different spectral ratios between P and S wave are expected that seismic velocities in the sediments (between the Earth surface and seismic bedrock) below the sites are continuously varied with depth, and have not clear discontinuity. Theoretical examination of vertical component ground motions excited by the obliquely incident S-wave pulse (incident angle=10˚) indicate that a spectral ratio of surface and borehole data in a continuous velocity model (mirage model) differs from one in a discontinuous velocity model (contrast model) (Fig. A). Difference of the spectral ratio in the contrast model between for the oblique incident S-wave and for the vertical incident P-wave indicates that the assumption of the P-wave incident in the previous studies is not reasonable for the continuous velocity structure. We examined vertical component ground motion recorded at TYMH02 KiK-net vertical array assuming a continuous velocity structure model. Although the synthetic waveforms at the surface from the borehole for the vertical incident P-wave indicated unacceptable monotonic waveforms, the synthetics for obliquely incident S-wave were comparable to the observed one (Fig. B).
Acknowledgement: KiK-net data was used.

Keywords: continuous velocity structure, oblique incident, S wave, vertical component

©2017. Japan Geoscience Union. All Right Reserved. 

## A) Theoretical examination

### 1) Structure model

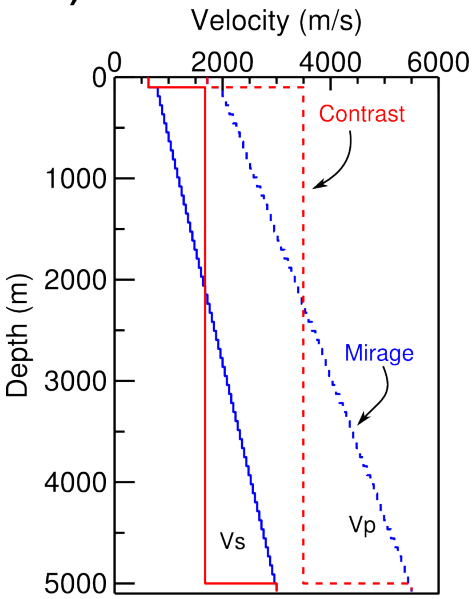


### 2) Waveform

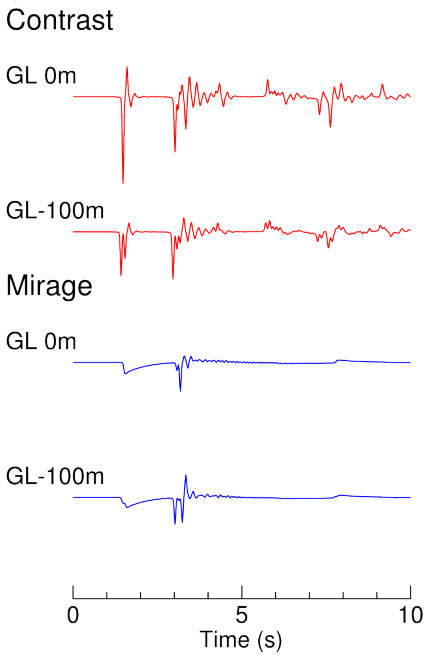


### 3) GL0m/GL-100m

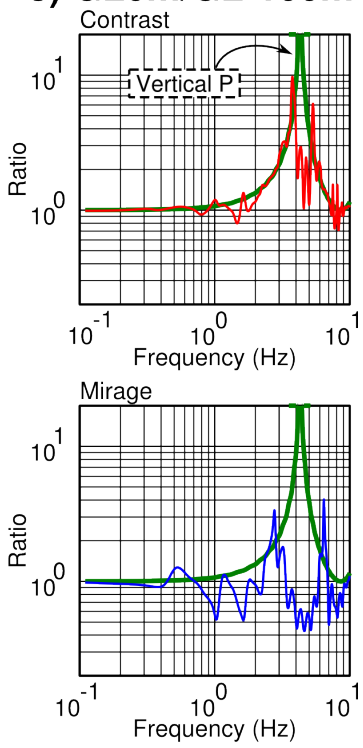


## B) TYMH02

### 1) Structure model

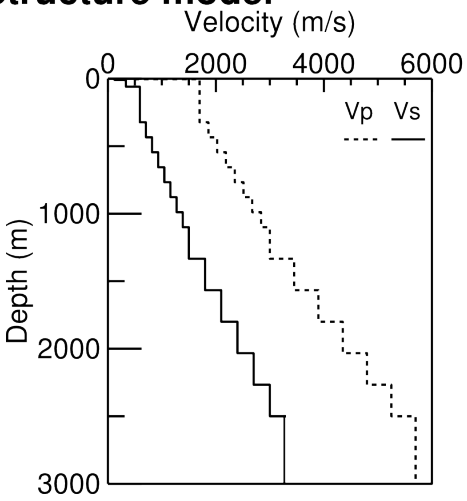


### 2) Waveform

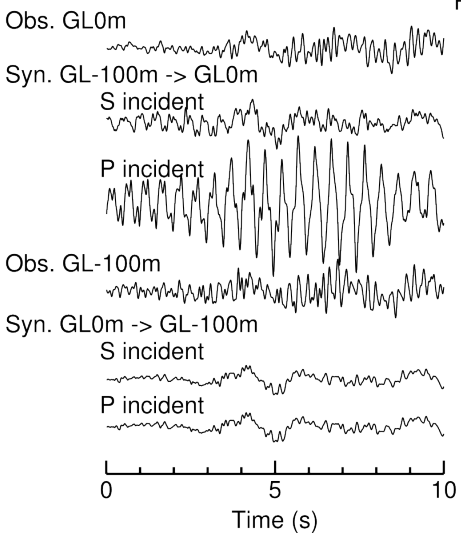


©2017. Japan Geoscience Union. All Right Reserved.

# Strong Ground Motion along the Joetsu Shinkansen during the 2004 Chuetsu Earthquake and Aftershock Sequence

*Yifei Chen[1], Hiroe Miyake[2]

1. GSII, The University of Tokyo, 2. III, The University of Tokyo

During the 2004 Chuetsu earthquake occurred at 17:56 on 23 October 2004, many relatively large-magnitude aftershocks occurred following the main shock (Mw 6.6). In the main shock, the seismic intensity meter of Kawaguchi-cho in Niigata prefecture recorded seismic intensity level 7, and equivalent seismic intensity level 7 was observed at K-NET Ojiya of NIED and Shinkawaguchi electrical substation of JR East (ARAIC, 2007). There were more than 10 earthquakes observed whose seismic intensity level were larger than 5+. All of them were observed in the areas such as Ojiya, Nagaoka, and Uonuma of Niigata prefecture. Large seismic intensity was observed in the watershed of the Shinano river where was near the epicenter and has a complex velocity structure with large site amplification factors.

During the 2004 Chuetsu earthquake, the first derailment of Shinkansen under operation ever occurred in which was slight south of the Nagaoka station of the Joetsu Shinkansen. The strong motion along the Joetsu Shinkansen has been discussed by Mori and Kazuni (2005), Nakamura (2006), and ARAIC (2007). Mori and Kazuni (2005) pointed out the influence of strong motion whose period was less than 0.5 second. On the other hand, the predominant period of the observed strong motion ranged from Ojiya to Nagaoka during the 2004 Chuetsu earthquake was 1 second. The 2004 Chuetsu earthquake and its aftershocks occurred in conjugated fault plane systems, both the hypocenter and velocity structures of which were complex. For that reason, it is difficult to obtain ground motion simulation results which are consistent with observation records. In this research, we focus on the arrival times of P-wave and S-wave for the 2004 Chuetsu earthquake and the importance of the distribution of strong ground motions. We also discuss the distribution of strong motion in the 2004 Chuetsu earthquake along the Joetsu Shinkansen by conducting ground motion simulation of aftershocks whose point-source assumption are easy to assume.

In the analysis, we deal with seismic intensity meters such as Niigata prefecture, JMA, K-NET, and KiK-net, using earthquake source models from F-net and Hikima and Koketsu (2005). We use J-SHIS as the initial velocity structure model. We also conduct ground motion simulation by using 3-D finite difference method from Aoi and Fujiwara (1999) in a period rang longer than 2 second and the stochastic Green’s function method by Dan and Sato (1998) in a period range shorter than 2 second. Calculation results are compared with the ground motion prediction equation of Si and Midorikawa (1999).

Keywords: 2004 Chuetsu earthquake, Joetsu Shinkansen, strong motion data, strong motion simulation

©2017. Japan Geoscience Union. All Right Reserved. 

# ERI Strong Motion Observation Network and Database

*Hiroe Miyake[1], Kazuki Koketsu[1], Takashi Furumura[1], Koji Miyakawa[1], Shinichi S Tanaka[1]

1. Earthquake Research Institute, University of Tokyo

Earthquake Research Institute, University of Tokyo (ERI) has performed strong motion observation since 1953, then currently operates the strong motion network with 64 stations. Most stations are located on the ground surface with K-NET95, and several stations with JEP-4B3 & SMAC-MDU or JEP-4B3 & AJE8200 are installed both at the borehole and the ground surface for better understanding of site response. Recently, we upgrade several stations in the rock tunnels and start continuous observation with JEP-8A3 & HKS9700 that can record distant earthquakes even occurred in the southern hemisphere. The data are transmitted to ERI every second via JDXnet by the mobile router for cell phones.

In addition to the Izu & Suruga bay, Ashigara valley, and southern Kanto regions, recently most offline stations are installed in the Nagano and Suwa basins as a framework of joint strong motion observation with Shinshu University. These stations are nearby the active fault traces such as the Itoigawa-Shizuoka tectonic line. The dominant periods of the Ashigara valley and the Suwa basin range between 1 to 3 s, that may affect largely on seismic intensity measures. The stations succeeded to record the 2009 Suruga-bay intraslab earthquake and the 2011 Tohoku megathrust earthquake. Strong azimuth variation along the coast line of the Suruga bay were captured during the 2009 Suguba bay earthquake, and significant local amplification in a period range of 2 to 3 s were seen in the Ashigara valley, rather than the Kanto basin during the 2011 Tohoku earthquake.

ERI established strong motion observation database in 2008. The data are open to the public via http://smsd.eri.u-tokyo.ac.jp/smad/ with K-NET format. Data of temporary strong motion observation by portable sensors after the 2004 Chuetsu, 2005 Fukuoka, 2007 Chuetsu-oki, and 2008 Iwate-Miyagi earthquakes are also open on the website with publications.

Keywords: strong ground observation network, database, temporary strong motion observation, joint strong motion observation, continuous observation

©2017. Japan Geoscience Union. All Right Reserved. 